AR-006-708

ELECTRONICS RESEARCH LABORATORY

Electronic Warfare Division

RESEARCH REPORT
ERL-0551-RR

ELECTRO-OPTIC DEVICES, COMPONENTS AND SYSTEM FOR THE MICROWAVE AND MILLIMETRE-WAVE RANGES

Dr. Yat Man CHOI

ABSTRACT (U)

Basic characteristics, performances and designs of integrated optic devices and components for use in microwave applications and various techniques for the microwave control of optical devices are reviewed. In particular, methods of improving their performances and limitations of such devices and components are discussed. The prospects for these new technologies including recommendations for further work which are relevant to microwave and millimetre wave systems are identified.

JUNE 1991

APPROVED FOR PUBLIC RELEASE

Postal Address: Director, Electronics Research Laboratory,
PO Box 1600, Salisbury, South Australia, 5108.

ERL-0551-RR

CONTENTS

1 INTRODUCTION 1
2 MICROWAVE/MILLIMETRE-WAVE CONTROLLED OPTICAL DEVICES 2
2.1 GaAs-based integrated opto-electronic circuits and devices 2
2.1.1 Laser diodes 2
2.1.2 Photodetectors 5
2.2 Ti:$LiNbO_3$ electro-optic modulators and switches 6
2.2.1 Interferometric modulator and switches 6
2.2.2 Switched directional coupler 8
2.2.3 Improved travelling-wave operation 9
2.2.4 Electrode impedance 11
2.2.5 Electrode attenuation 12
2.2.6 Coupling loss between a single-mode optical fiber and a channel waveguide 12
2.3 Fiber-optic delay lines 12
3 MICROWAVE FIBER-OPTIC LINKS 13
3.1 Direct modulation link 14
3.1.1 Insertion loss 14
3.1.2 Laser modulation bandwidth 15
3.1.3 Relative intensity noise (RIN) 16
3.1.4 Equivalent input noise (EIN) 17
3.1.5 Link noise 17
3.1.6 Noise figure 20
3.1.7 Dynamic range 20
3.2 External modulation link 22
3.2.1 Insertion loss 22
3.2.2 Noise figure 23
3.2.3 Link bandwidth 23
4 SUGGESTIONS FOR FUTURE WORK RELEVANT TO OPTICAL MICROWAVE/ MILLIMETRE-WAVE INTERACTIONS 23
4.1 Modulator 24
4.2 Switch 25
4.3 Oscillator 25
4.4 Amplifier 25
4.5 Detector 25
4.6 Filter 26
4.7 Fiber-optic delay line 26
4.8 Fiber-optic link 26
5 CONCLUSIONS 26
ACKNOWLEDGEMENTS 26
REFERENCES 27

LIST OF TABLES

1 Material comparisons for optical circuits....1
2 Coupling efficiencies between lasers and single-mode optical fiber....3
3 Linear electro-optic coefficients of $LiNbO_3$....11
4 Performance comparison of directly modulated and externally modulated microwave fiber-optic links....13

LIST OF FIGURES

1 Techniques to couple a semiconductor laser diode to a single-mode optical fiber: (a) hemispherical micro-lens; (b) conical lens; (c) spherical lens; (d) tapered fiber with high-index lens; (e) direct coupling (butt coupling)....3
2 Light output versus the laser diode current....4
3 Interferometers: (a) Y-branch and (b) Mach-Zehnder....8
4 Switched directional coupler....9
5 Reversed-$\Delta\beta$ directional coupler switch....9
6 Travelling-wave modulator using a coplanar strip electrode with shielding over plane....11
7 Schematic of a travelling wave modulator with periodic reversal electrodes....11
8 An asymmetric coplanar stripline electrode structure....12
9 Simplified laser link equivalent circuit for link loss calculation....15
10 Typical frequency response of a laser diode....16
11 Laser light-current (L-I) curve....17
12 Total EIN versus optical loss. Typical performance for the Ortel 3510B/4510B link....19
13 Total EIN versus optical loss. Typical performance for the Ortel 5515A 10 GHz link....20
14 A typical illustration of second- and third-order intermodulation product levels, intercept points, noise floor, and SFDR for a hypothetical microwave fiber-optic link....22
15 Schematic of an externally modulated analog fiber-optic link for microwave transmission....23

1 INTRODUCTION

In the past few years tremendous strides have been made in the realization of microwave monolithic integrated circuits (MMICs) for communications, radar and high-speed digital applications [1]. In particular, discrete field-effect transistors with unity current-gain cutoff frequency (f_t) greater than 125 GHz [2] and noise figure and gain of about 1.5dB and 6dB respectively at 94 GHz have been achieved. Special IMPATT (impatt avalanche and transit time) diode [3] and PIN (positive-intrinsic-negative) diode [4] structures suitable for monolithic integration as well as for efficient coupling of light into the device active region have also been made.

Concurrently, there has been considerable progress made in the development of opto-electronic devices such as:

1. laser diodes with relaxation frequencies as high as 30 GHz [5],
2. photodetectors with bandwidth greater than 100 GHz [6] and
3. electro-optic intensity modulators with bandwidths of the order of up to 40 GHz [7],[8].

Advances in fabrication and processing techniques [9] should eventually lead to further improvements in design and reduction of parasitic capacitances, thereby extending the upper limit of bandwidth into the millimetre-wave region.

Optical waveguides, components and devices have been fabricated in various materials, using a variety of techniques. $LiNbO_3$ has been used to realize many integrated optics (IO) devices except emitters and detectors. Silicon or gallium arsenide (GaAs) are the chosen materials for higher levels of integration of IO. Table 1 shows a comparison of the semiconductor and $LiNbO_3$ technology [10].

Table 1 Material comparisons for optical circuits.

Property	$LiNbO_3$	GaAs/AlGaAs	Thin film on silica
Form	Single crystal	Epitaxially grown	Thin-film evaporation or sputtering
Refractive index	2.2	3.5	Depends on Materials (ZnO and Si_3N_4, n = 2)
Attenuation	0.5 dB/cm	1-2 dB/cm, λ = 1.3 μm 5 dB/cm, λ = 0.85 μm	0.1 dB/cm
Birefringence	Very high	Low	High
Electro-optic coefficient	High $r_{33} = 30 \times 10^{-12}$ m/V	Medium $r_{33} = 1.5 \times 10^{-12}$ m/V	Medium $r_{33} = 2 \times 10^{-12}$ m/V (ZnO)
Piezoelectric	Good	No (but techniques exist for generating acoustic waves)	Material dependent—yes for ZnO
Electronic compatibility	No	Yes	Yes
Laser compatibility	No	Yes	No

In this report, designs of integrated optics devices and components and various techniques for the microwave control of optical devices are reviewed. In addition, the basic equations of insertion loss, noise contributions, dynamic range, etc. for both directly and externally modulated fiber-optic links are

presented. The prospects for these new technologies including recommendations for future work relevant to microwave and millimetre wave systems are discussed. Several of these techniques have not yet been demonstrated in the monolithically integrated form, but they have been demonstrated in discrete or hybrid configurations. Nevertheless, the same basic principles apply, and monolithic integration will inevitably follow.

2 MICROWAVE/MILLIMETRE-WAVE CONTROLLED OPTICAL DEVICES

2.1 GaAs-based integrated opto-electronic circuits and devices

GaAs and InP (III-V materials) can emit light and therefore it becomes possible to integrate optical emitters on the IC to perform the I/O (input/output) functions.

2.1.1 Laser diodes

(A) Coupling to a single-mode optical fiber

Figure 1 illustrates several methods [11] of coupling between a semiconductor laser and a single-mode fiber. The measured coupling efficiency in each case is summarised in Table 2 [11].

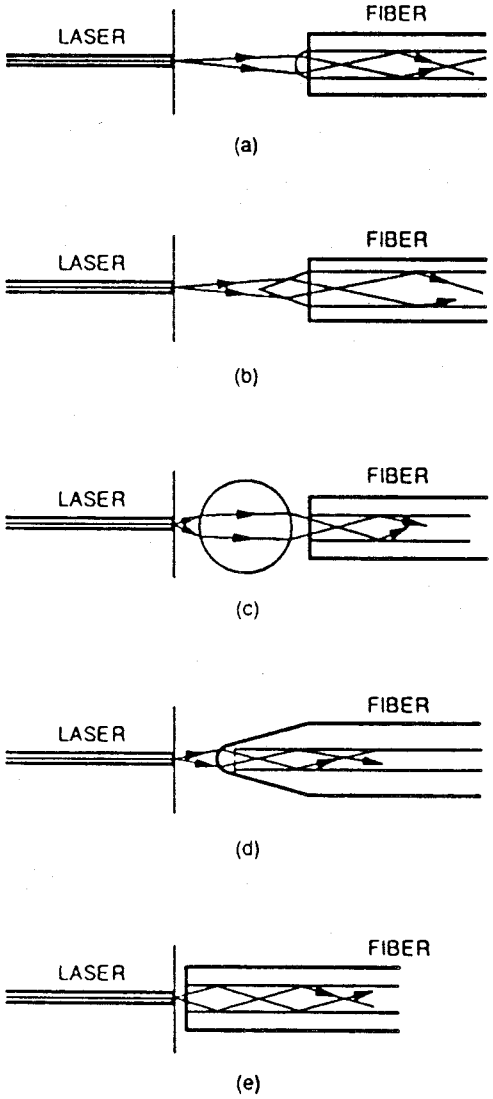

Figure 1 Techniques to couple a semiconductor laser diode to a single-mode optical fiber: (a) hemispherical micro-lens; (b) conical lens; (c) spherical lens; (d) tapered fiber with high-index lens; (e) direct coupling (butt coupling).

Table 2 Coupling efficiencies between lasers and single-mode optical fiber.

Laser Type and Wavelength	Fiber Type and Core Diameter	Method of Coupling	Coupling Loss (dB)
(InGaAsP Buried-Heterostructure, 1.3 μm)	Single-Mode 8 μm	Hemispherical Microlens	2.9
	Single-Mode 8 μm	Conical Lens	3.0
	Single-Mode 10 μm	Spherical Lens	4.0
	Single-Mode	Tapered Fiber with High-Index Lens	2.6
	Single-Mode 8 μm	Butt Coupling	>10.0

(B) Direct current modulation of semiconductor lasers

Figure 2 shows the relative light output from a semiconductor laser versus the laser diode current. By injecting the modulating microwave signal along with the dc bias, the laser diode output can be directly intensity-modulated.

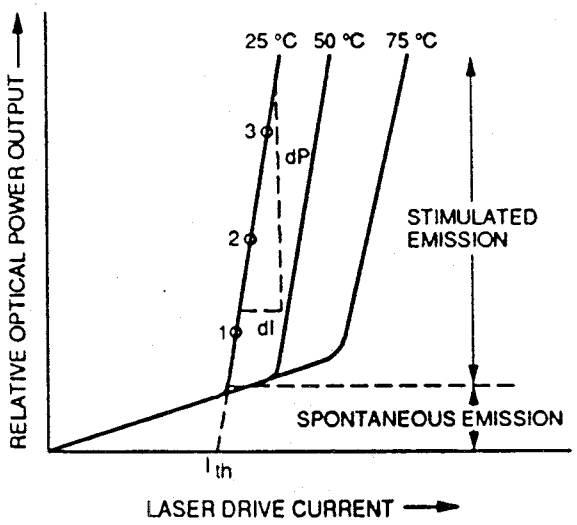

Figure 2 Light output versus the laser diode current.

Starting from the rate equations inside the laser medium [11], an expression for the peak frequency (known as the relaxation frequency and denoted as ω_r) is obtained:

$$\omega_r = \{A * P_o / t_p - (1/2) * [1/t + A * P_o]^2\}^{1/2} \quad (1a)$$

$$= \{A * P_o / t_p\}^{1/2} \quad (1b)$$

$$= \{(1 + A * t_p * \Gamma * N_{tr}) / (t * t_p) * (I_o / I_{th} - 1)\}^{1/2} \quad (1c)$$

where

A = optical gain coefficient;

P_o = photon density inside the active region of a semiconductor laser diode at steady-state (dc condition);

t_p = photon lifetime as limited by the absorption in the bounding medium, scattering, and coupling through the output mirrors;

t = spontaneous recombination lifetime;

Γ = confinement factor;

N_{tr} = inversion density needed to achieve transparency (ie, the electron density in the medium must exceed a certain level to exhibit positive gain);

I_o = total steady-state (dc) current; and

I_{th} = threshold current.

It can be seen from Equation 1 that, the modulation bandwidth can be increased by:

1. Increasing the gain coefficient A (by a factor of 5), by cooling the laser from room temperature to liquid nitrogen temperature of 77°K [12]. This temperature dependent characteristic causes the lasing threshold current to change exponentially as the temperature changes. This is approximated by the equation

$$I_{th}(T) = I_{th}(25°C) * \exp[(T - 25°C)/T_o] \quad (1d)$$

where $I_{th}(25°C)$ is the threshold current at 25°C; and

T_o is the characteristic temperature of the laser and has a value between 100° and 300°C, depending on the laser structure and materials.

As an example, the measured bandwidth of a typical InP/InGaAsP constricted-mesa laser is about 16 GHz at room temperature. By cooling the laser to -60°C, the observed bandwidth increases to 26.5 GHz [11].

2. Increasing the photon density P_o in the active region by biasing the laser at higher currents. However, catastrophic mirror damage occurs at a power density of about 1 MW/cm^2, for a laser with a mirror reflectivity of 0.3 [12],[13]. This sets an upper limit on the maximum permissible photon density, and hence the maximum modulation bandwidth. This limit can be increased by incorporating a window structure [14].

3. Reducing the photon lifetime t_p by decreasing the laser cavity length. Such a laser has to operate at a higher current density, and therefore, thermal effects due to heating will limit the maximum attainable modulation bandwidth. As an example, a laser with a cavity length of 300 μm operating at an output optical power density of

0.8 MW/cm^2 possesses a bandwidth of 5.5 GHz, and corresponding pump current density is 3 kA/cm^2. Reducing the cavity length to 100 μm and operating at an identical power level results in a bandwidth of 8 GHz, but the corresponding current density is 6 kA/cm^2 [12]. The thermal effects alone may cause the laser to degrade rapidly.

4. Increasing the dc component of the current I_0.

The fabrication of semiconductor laser diodes requires crystal growth and processing steps similar to IC manufacture in order to define the electrical and optical cavity in the two dimensions perpendicular to the direction of light propagation. The length of the cavity is defined by the partial mirrors which are formed by cleaving the semiconductor along parallel crystal planes.

The operation of the laser diode is achieved using current instead of voltage. The gain medium is achieved by driving a current across a p-n junction which inverts the carrier population in the active region. Therefore, the diode requires electrical connections to two contacts. The inversion is aided by the growth of heterostructures near the p-n junction which provide barriers to the injected minority carriers, confining them to very narrow regions. The heterostructure also produces an optical waveguide due to a change in the index of refraction between the two materials.

The integration of the laser with the associated electronics will be limited by the materials and processing compatibility. There are three major reasons for this:

1. lasers require a multilayered heterostructure up to 7 μm thick;
2. they need two parallel mirrors at about 200 μm separation; and
3. a method is needed that can achieve electrical and optical confinement in the lateral dimension

It is beyond the scope of this paper to discuss the operational characteristics required for laser diodes and the types of lasers that can meet these characteristics.

2.1.2 Photodetectors

Primarily, three types of detectors have received attention for integration applications. These are PIN diodes, avalanche photodiodes (APDs), and photoconductive detectors. The integration of the detector and the pre-amplifier into an optical receiver will result in the reduction of the parasitic capacitance of the circuit.

A useful comparison of these detectors can be made by considering how their choice influences the performance of an RF fiber optic link. At bit rates below 4 Gb/s, the APD offers the best performance [11].

(A) PIN receiver

The reduction of the circuit parasitic capacitance could result in an improvement in the sensitivity of the receiver to the level where it is comparable to the photoconductive receiver.

Reference [11] showed that a given semiconductor material is usable only over a limited wavelength range. In addition, the frequency response of PIN photodiodes is limited by three factors:

1. the time it takes for carriers generated outside the depletion region to diffuse to the depletion region;

2. the time required for photo-injected carriers to drift across the depleted layer; and

3. the RC time constant determined by the inherent junction capacitance of the structure and the equivalent resistance of the diode and the external circuit.

Hence, for high-speed operation, the depletion layer should be thin so that the transit time is short, and the diode area should be small for small capacitance. However, a very thin depletion layer will decrease the absorption of radiation, and thus diminish the quantum efficiency. A small device area makes difficult fabrication as well as light injection. Thus, the design of a very high-speed photodiode involves compromise.

(B) APD receiver

This receiver has the highest sensitivity. However, the high voltage required is not compatible with many applications and it would be extremely difficult to electrically isolate the high voltage from the electronics. In addition, the avalanche gain is temperature dependent and would require extra expense to stabilize.

The APD has an optimal gain for which the signal-to-noise ratio is maximised. In the presence of the gain, the bandwidth is reduced because time is taken for an avalanche to build up.

(C) Photoconductive receiver

This receiver is limited by the noise of the photoconductive channel rather than by circuit parasitics, and therefore, it would gain little sensitivity from integration. On analysis, it can be shown that they will be slower than PIN detectors. However, they are extremely easy to fabricate and will be more cost effective and reliable to integrate than a PIN diode.

The gain of photoconductive detectors is proportional to the ratio of the hole lifetime to the electron transit time. Because the hole lifetime is greater than the electron transit time, the holes continue to drift, even after the end of the optical pulse. This increases the detector response time. Because the response time and the bandwidth are inversely proportional, any increase in the gain is at the expense of the bandwidth. The signal-to-noise ratio increases with decreasing dark conductance G or increasing gain. However, any increase in gain to improve sensitivity decreases the frequency response.

2.2 Ti:$LiNbO_3$ electro-optic modulators and switches

In this case, a cw laser source is modulated by exploiting the electro-optic effect, that is, the change in refractive index that occurs in some crystals when subject to an electric field. The changing refractive index, caused by the microwave signal, is used to phase modulate the cw laser beam. This phase modulation is converted to an intensity modulation. The design and performance of these devices are given in the next section.

For a given electrode length, the achievable bandwidth is critically dependent on the mismatch between the optical and microwave velocities [11] which can be reduced by techniques as given in Section 2.2.3.

2.2.1 Interferometric modulator and switches

The design and performance of the Y-branch and Mach-Zehnder electro-optic travelling wave modulators have been reported by several investigators [15],[16]. Figure 3 shows the two versions of interferometric-type modulators.

Assuming perfect 3dB splitting and combining for the Mach-Zehnder and Y-branch interferometers, the transfer efficiency or intensity transmittance is given by

$$\eta = \cos^2(\Delta\beta * L / 2) \qquad (2)$$

where

$\Delta\beta$ = $(2\pi / \lambda) * \Delta N_{eo}$;

ΔN_{eo} is electro-optically induced index difference between the two interferometer arms;

λ is the free-space wavelength; and

L is the interaction length between the two interferometer arms.

The optical power that can be delivered to the device is limited by photo-refractive damage to the electro-optical material and, if single-mode fiber is used at the input, the onset of non-linear processes in the input fiber. The problem of photo-refractive damage is severe at visible wavelengths, however, at the preferred communications wavelengths of 1.3 μm and 1.5 μm, the problem is drastically reduced. For example, while 3.2 μW of power at 850 nm can cause photo-refractive damage, it requires > 0.5 mW at 1300 nm and > 75 mW at 1500 nm. However, the modulator has the advantage that its response which is highly non-linear, is frequency independent.

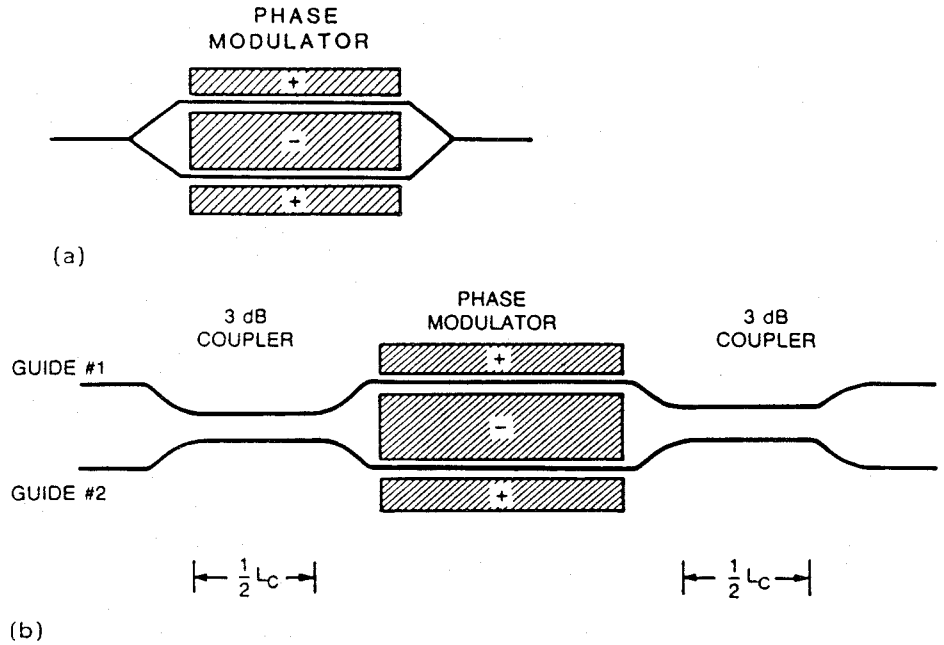

Figure 3 Interferometers: (a) Y-branch and (b) Mach-Zehnder.

2.2.2 Switched directional coupler

This is an optical circuit device for both on/off modulation and switching, and is based on adjustable phase mismatch, shown schematically in Figure 4.

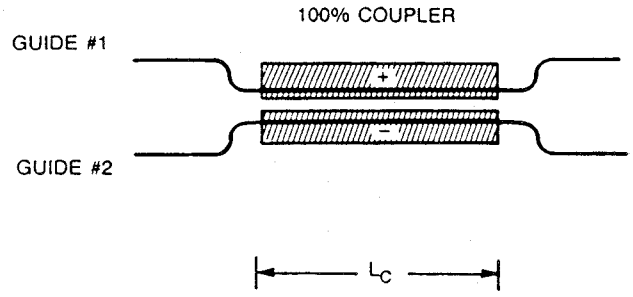

Figure 4 Switched directional coupler.

The cross-over efficiency, η, is given by [10]:

$$\eta = \frac{\sin^2 \kappa L\left[1+(\delta/\kappa)^2\right]^{1/2}}{1+(\delta/\kappa)^2} \qquad (3)$$

where κ is a local coupling coefficient between the two waveguides;
δ = $\Delta\beta / 2$;
$\Delta\beta$ = $(2\pi / \lambda) * |N_2 - N_1|$ of the two waveguides;
L = interaction length between the two interferometer arms;
λ = free-space wavelength;
N_1 = refractive index of arm 1 of the waveguide interferometer; and
N_2 = refractive index of arm 2 of the waveguide interferometer.

Complete electrical control over both switch states for much more flexible fabrication tolerance can be achieved by using a split-electrode design - referred to as the $\Delta\beta$-reversal electrode [10] - shown in Figure 5.

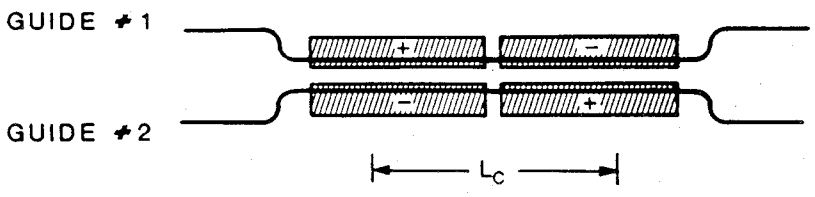

Figure 5 Reversed-$\Delta\beta$ directional coupler switch.

The transfer efficiency for the reversed-$\Delta\beta$ coupler of N sections (N even) can be written simply as [10]:

$$\eta_{\Delta\beta} = \sin^2 \kappa_{eff} L \tag{4}$$

where $\kappa_{eff} = (N/L) \sin^{-1} \sqrt{\eta}$; and

η is the cross-over efficiency for one section of length L/N, as given by Equation (3).

2.2.3 Improved travelling-wave operation

For most practical wave-guide modulators, the velocities of the lightwave and the microwave are not matched with each other, and their bandwidths are limited by the velocity mismatch. With a reduced interaction length, L_i, faster operation will be achieved, although higher drive power is required since the power is proportional to $1/(L_i^2)$. A way to realize efficient, fast and wide-band operation at the same time is to reduce the velocity mismatch between light and modulating waves. The following methods serve to reduce their velocity mismatch:

(A) A groove is etched between the parallel optical waveguides. The groove decreases the index of refraction at microwave frequencies and hence improves the match [17].

(B) The use of a shielding ground plane above the coplanar strip on $LiNbO_3$ substrate [18] (Figure 6). With this structure, efficient modulation was performed over 20 GHz.

(C) Use of an extremely thick (7 to 9 μm) electrode [19].

(D) Use of the ridge waveguide structure [20].

(E) Periodic loading of the capacitance between modulator electrodes has been used to form a slow-wave structure for the GaAs travelling-wave modulator [21] wherein the modulating wave is faster than the light wave.

(F) The electrodes are shifted after an interaction length L_i so that the direction of the applied field in the waveguide is reversed as shown in Figure 7. The value of L_i is chosen such that this field direction reversal exactly compensates for the polarity reversal caused by the difference between the phase velocities of the optical and microwave signals at a design frequency f_d [22]. Applying a special sequence for the reversal (instead of a periodic one) of the modulation polarity can result in broad-band operation; bandwidths up to 40 GHz have been reported [7],[8].

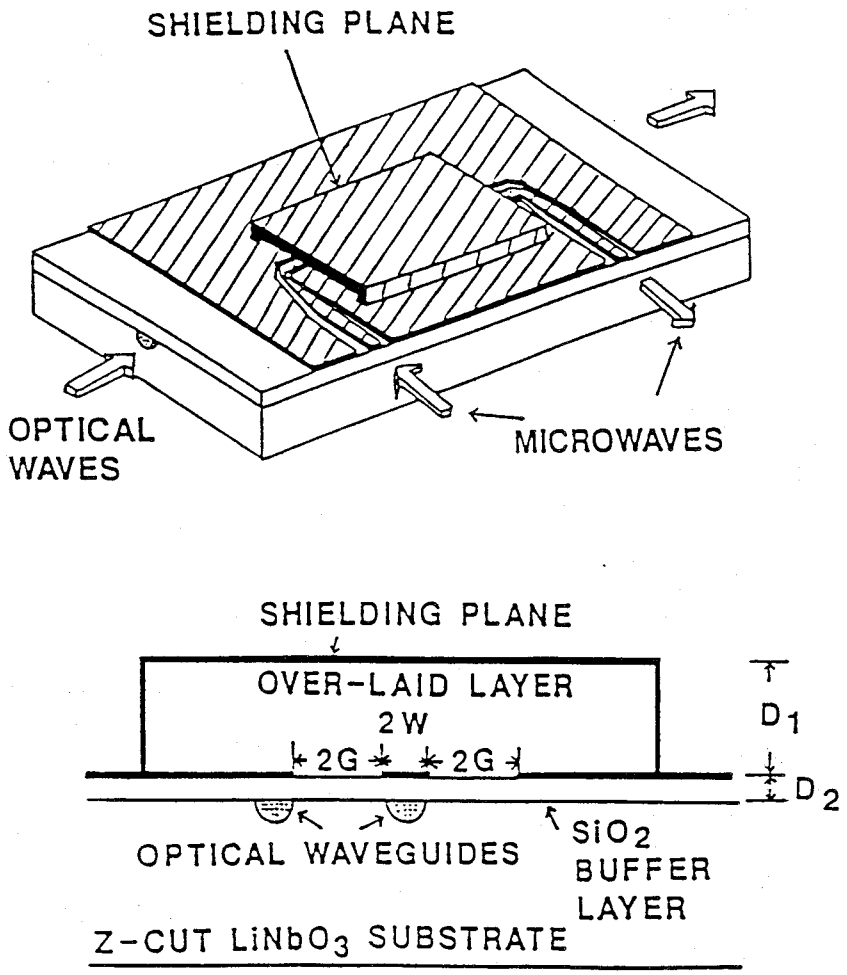

Figure 6 Travelling-wave modulator using a coplanar strip electrode with shielding over plane.

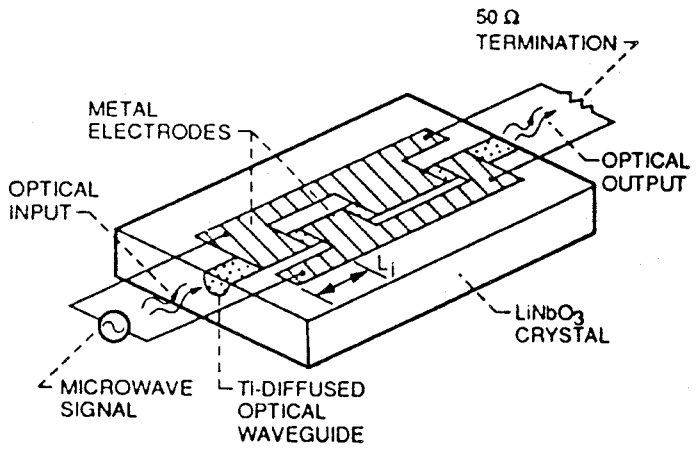

Figure 7 Schematic of a travelling wave modulator with periodic reversal electrodes.

2.2.4 Electrode impedance

The characteristic impedance is given by [23]:

$$Z_o = [240\pi / (\varepsilon_{eff})^{1/2}] * [K(t_a) / K(t_b)] \quad (5)$$

where $t_a = [G/(2W+G)]^{1/2}$

$t_b = [1 - t_a^2]^{1/2}$;

ε_{eff} = effective dielectric constant

$= [1 + (\varepsilon_{||} * \varepsilon_{\perp})^{1/2}] / 2$;

and W, G are defined in Figure 8. $K(t_a)$ and $K(t_b)$ are the complete elliptic integral of the first kind. The values of $\varepsilon_{||}$ and $\varepsilon_{\perp}$ can be found in Table 3.

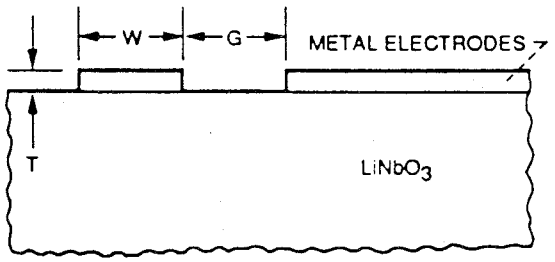

Figure 8 An asymmetric coplanar stripline electrode structure.

Table 3 Linear electro-optic coefficients of $LiNbO_3$.

Symmetry	Pockels Constants X 10^{-12} (m/V) [a]	Refractive Index	Wavelength Range for Transparency (μm)	Specific Dielectric Constants [c]	Curie Temperature (°C)	Temperature Coefficient of the Refractive Indices [d] ($\delta n/\delta T$) X 10^{-5}
3m	$r_{33} = 30.8$	$n_o = 2.286$[a]	0.4 - 5	$\varepsilon_{\perp} = 43$	1470	n_e : +5.3
	$r_{13} = 8.6$	$n_e = 2.200$[a]		$\varepsilon_{||} = 28$		n_o : +0.56
	$r_{22} = 3.4$	$n_o = 2.237$[b]				
	$r_{51} = 28$	$n_e = 2.157$[b]				

[a] At $\lambda = 0.6328$ μm, room temperature under constant strain.
[b] At $\lambda = 1.0$ μm.
[c] $\varepsilon_{\perp}$ and $\varepsilon_{||}$ are values normal and parallel to the crystal axis, respectively.
[d] Over the temperature range of 20-40°C.

2.2.5 Electrode attenuation

At frequencies where the skin depth, d, is much less than the electrode thickness, T, the sheet resistance, R_S, of the electrode metalization is expressed as [24]:

$$R_S \cong \frac{1}{d\sigma} = \sqrt{\frac{\pi\mu}{\sigma} * f} \tag{6a}$$

where σ = conductivity;
μ = permeability of the metal; and
f = operating frequency.

At low frequencies, where the skin depth is large compared to the electrode thickness, R_S is approximated by:

$$R_S \cong 2 / (\sigma * T) \tag{6b}$$

2.2.6 Coupling loss between a single-mode optical fiber and a channel waveguide

The coupling efficiency can be calculated using [25]:

$$\eta = \frac{2\left[(1/a^2 + 1/W_a^2)^{-1/2} + (1/a^2 + 1/W_s^2)^{-1/2}\right]^2}{a^2 W_p (W_a + W_s)(1/a^2 + 1/W_p^2)} \tag{7}$$

where

a = mode size of the single-mode fiber;
W_a = upper half of the waveguide mode depth;
W_s = lower half of the waveguide mode depth;
W_p = width of the waveguide mode;
r = W_a / W_s = depth mode asymmetry ratio;
γ = $W_{\|} / W_{\perp}$ = waveguide mode eccentricity;
$W_{\|}$ = $2 W_p$ = full width at the intensity 1/e point; and
$W_{\perp}$ = $W_a + W_s$ = depth at the intensity 1/e point.

2.3 Fiber-optic delay lines

The use of fiber-optic components and topologies for delay line applications are discussed in Reference [26],[27]. System considerations including dispersion and noise accumulation were also discussed.

3 MICROWAVE FIBER-OPTIC LINKS

Microwave fiber-optic communication links have several advantages when compared to conventional coaxial and waveguide links. The advantages are:

1. greatly reduced size and weight;
2. as the number of transmission paths increases, the weight saving obtained with optical fiber cable increases, dramatically;
3. low and constant attenuation over the entire modulation frequency range;
4. impervious to electromagnetic interference (EMI), radio frequency interference (RFI), and electromagnetic pulse (EMP);
5. wide bandwidth; and
6. high information transfer capacity.

Applications of fiber-optic links include radar, communication, signal processing and remote sensing.

In general, microwave fiber-optic communication links are of two types [28],[29]. They are:

1. direct modulation link; and
2. external modulation link.

A performance comparison is given in Table 4 and limitations, relations with technical requirements and prospects for future enhancements of link performance parameters relating to signal-to-noise ratio, bandwidth, insertion loss and dynamic range will be discussed.

Table 4 Performance comparison of directly modulated and externally modulated microwave fiber-optic links.

	Directly Modulated	Externally Modulated
Laser Transmitter Type	1.3μm, InGaAsP, BH	1.3μm, InGaAsP, BH
Photodiode Receiver Type	PIN, InGaAs	PIN, InGaAs
Modulator Type	—	Mach-Zehnder on $LiNbO_3$
Fiber Type and Length	single-mode, 1.1 km	single-mode, 1 km
Laser RIN (dBm/MHz)	-59.7	-66.0
Bandwidth (GHz)	4.1 to 4.7	2.0 to 12.0
Input Level (dBm)	0	0
Signal-to-noise Ratio at Output in 1 MHz Bandwidth (dB)	59.3	53
Link Loss (dB)	36.4	67
Dynamic Range at Output in 1 MHz Bandwidth (dB)	44	—
Third-Order Intermodulation Product Suppression (dBc)	-36	—
Insertion Loss of Modulator (dB)	—	7
Voltage for 100% Modulation (V rms)	—	7.6

3.1 Direct modulation link

3.1.1 Insertion loss

Figure 9 shows a simplified laser link equivalent circuit for link loss calculation. The input impedance R_{in} includes the laser diode impedance and any input matching impedance. The laser output optical power coupled into the fiber is indicated by P_{laser} whereas the optical power incident on the photodiode is shown as P_{pd}. The photodiode is shown as a current source. The module output impedance R_o is the parallel combination of the photodiode impedance (1 to 2 k-ohms) and the output matching resistor (50 ohms is the standard). Details of the equivalent circuit such as photodiode junction capacitance and lead resistance and inductance are not shown.

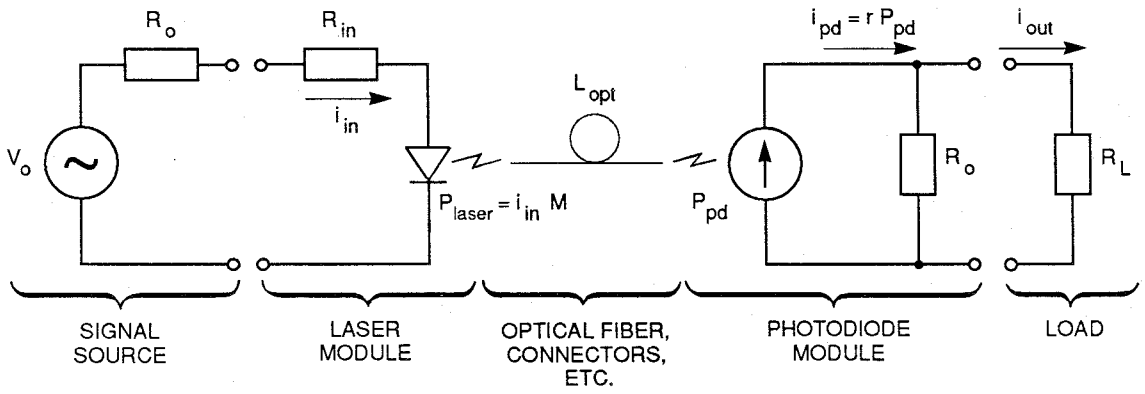

Figure 9 Simplified laser link equivalent circuit for link loss calculation.

It has been shown that the link insertion loss [30], L_{link}, can be written as:

$$L_{link} = 1/G_{link}$$

$$= \left[\frac{R_o + R_L}{R_o} * \frac{L_{opt}}{r*M}\right]^2 * \frac{R_{in}}{R_L} \qquad (8)$$

$$= 20\log\frac{R_o + R_L}{R_o} + 2L_{dB} + 10\log\frac{R_{in}}{R_L} \quad (dB)$$

where

G_{link} is the delivered power gain of the link;

R_{in}, R_o and R_L are the respective input, output and load impedance as defined in Figure 9;

L_{dB} = 10*log(L_{opt}) is the optical loss in the fiber and the connectors given in dB;

r is the responsivity which converts incident optical power to photodiode output current (mA/mW); and

M is the modulation gain which combines the quantum efficiency and the fiber coupling efficiency into this single specification. This factor converts input current to laser optical power coupled into the fiber (mW/mA).

Typical values of M, r, R_o, R_L and R_{in} are

M = 0.04 mW/mA;

r = 0.6 mA/mW;

$R_o = R_L$ = 1 k-ohms; and

R_{in} = 5 ohms.

With normal fiber coupling (15%) and L_{dB} = 0, Insertion Loss = 15.4 dB for a link which is reactively matched perfectly at the input and output.

3.1.2 Laser modulation bandwidth

The link bandwidth is determined by the low and the high frequency limits of the laser diode frequency response [31] for a directly modulated system. The low frequency limit is set by the cut-off frequency of the low-pass filter in the laser diode bias tee. The high frequency limit is set by the roll off in the frequency response of the laser diode , which has a typical slope of 40 dB/decade beyond the relaxation oscillation frequency. This characteristic is illustrated in Figure 10. Most microwave applications require a narrow bandwidth typically less than 500 MHz [31], although applications involving bandwidths to 20 GHz are of interest. Commercially available laser diodes are capable of being directly modulated at frequencies of up to 10 GHz [32]. Laboratory experimental laser diodes with a relaxation frequency as high as 30 GHz have been recently demonstrated [5].

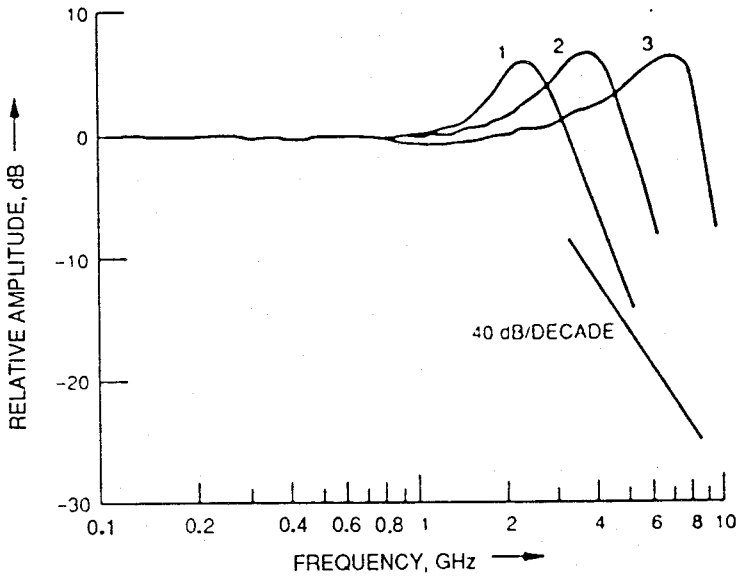

Figure 10 Typical frequency response of a laser diode.

Theoretical analysis shows that the intrinsic modulation response of a semiconductor laser behaves as a second order low-pass network exhibiting a resonance peak before rolling off at 40 dB/decade at high frequencies. The 3 dB modulation bandwidth f_{3dB} of a laser follows the relationship

$$f_{3dB} = A\,[P_{out}]^{1/2} \qquad (9)$$

where A is a constant and P_{out} is the average CW optical output power of the laser. Since P_{out} is a linear function of the laser bias current, one can see that the modulation bandwidth is increased by increasing the laser bias. Increasing the laser bias also increases the available dynamic range (clipping occurs at higher RF power levels). The practical upper limit is determined by linearity requirements, diode and packaging parasitics and reliability. When the laser bias is increased, it also runs hotter, which reduces its mean time to failure (MTTF). Because of these considerations, not all lasers which perform to specification at 3 GHz will meet specification at higher frequencies such as 6 and 10 GHz.

3.1.3 Relative intensity noise (RIN)

The laser RIN is defined as

$$RIN = \frac{<\Delta P^2>}{P_o^2} * \frac{1}{B} \quad (dB/Hz) \tag{10}$$

where $<\Delta P^2>$ is the mean square power fluctuation in the output;
P_o^2 is the square of the mean power; and
B is the bandwidth.

These fluctuations are due to the shot noise processes associated with carrier injection and recombination within the active layer. For analog communications, a laser is DC biased in the middle of its linear region as shown in Figure 11.

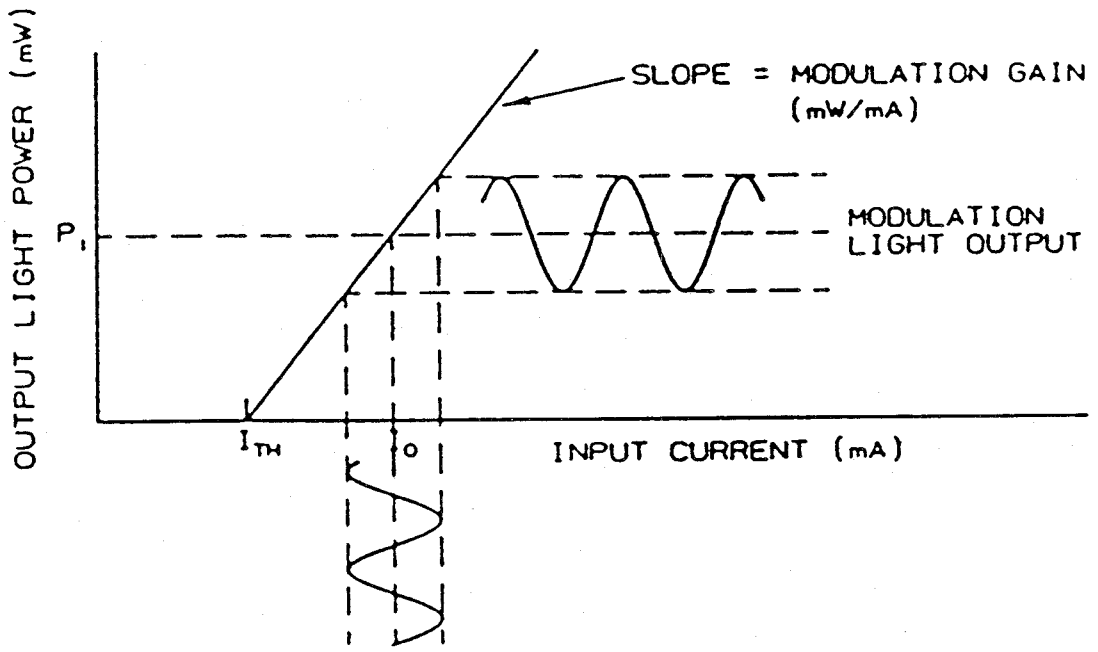

Figure 11 Laser light-current (L-I) curve.

Now, the laser converts input current to output optical power. Since we are operating in the linear region of the L-I curve, this conversion factor is a constant - namely, the modulation gain, M.

Therefore,

$$RIN = \frac{<\Delta I^2> M^2(f)}{(I - I_{th})^2 M^2(0)} * \frac{1}{B} \quad (dB / Hz) \tag{11}$$

where

M(f) indicates the frequency dependence of the effective modulation gain;

M(0) is the DC modulation gain;

$<\Delta I^2>$ is the mean square of the input current fluctuations that would produce the observed output light intensity fluctuations if the laser itself were noiseless;

I is the total current; and

I_{th} is the threshold current.

The frequency dependence of the modulation gain, M(f), could be found by measuring the link loss as a function of frequency using a photodiode with a known responsivity, r, connected to the laser with a fixed optical loss, L_{opt} and using Equation 8 to compute M(f).

3.1.4 Equivalent input noise (EIN)

The laser EIN is defined as

$$EIN = <\Delta I^2> * R_i * \frac{1}{B} \quad (Watts / Hz) \tag{12}$$

where $<\Delta I^2> * R_i$ is the electrical noise power due to the mean square of the input current fluctuations, $<\Delta I^2>$, across the input impedance, R_i, of the RF input circuit including the laser diode.

From Equations 11 and 12,

$$EIN = RIN * (I - I_{th})^2 * R_i * \frac{M^2(0)}{M^2(f)} \quad (Watts / Hz) \tag{13}$$

3.1.5 Link noise

The total equivalent input noise of a fiber-optic link is made up of three components [30]:

(1) laser noise, EIN_{laser};

(2) photodiode shot noise, EIN_{shot}; and

(3) receiver thermal noise, $EIN_{thermal}$.

ie $$EIN = EIN_{laser} + EIN_{shot} + EIN_{thermal} \tag{14}$$

where

EIN_{laser} is given by Equation 13 (Watts/Hz) (14a)

$EIN_{shot} = 2\,e\,r\,P_{pd}\,[R_o/(R_o+R_L)]^2\,R_L\,L_{link}$ (Watts/Hz) (14b)

$EIN_{thermal} = k\,T\,L_{link}$ (Watts/Hz) (14c)

e = electric charge = $1.6 * 10^{-19}$ Coul;
r = photodiode responsivity in A/Watt;
P_{pd} = optical power incident on the photodiode;
R_o = photodiode module output resistance;
R_L = load resistance;
L_{link} = electrical loss of the link;
k = Boltzmann's constant = $1.38 * 10^{-23}$ Watts/Hz; and
T = absolute temperature in °K.

Figures 12 and 13 show the total EIN versus Optical loss, L_{opt}, using typical values for the Ortel 3510B/4510B and 5515A link respectively.

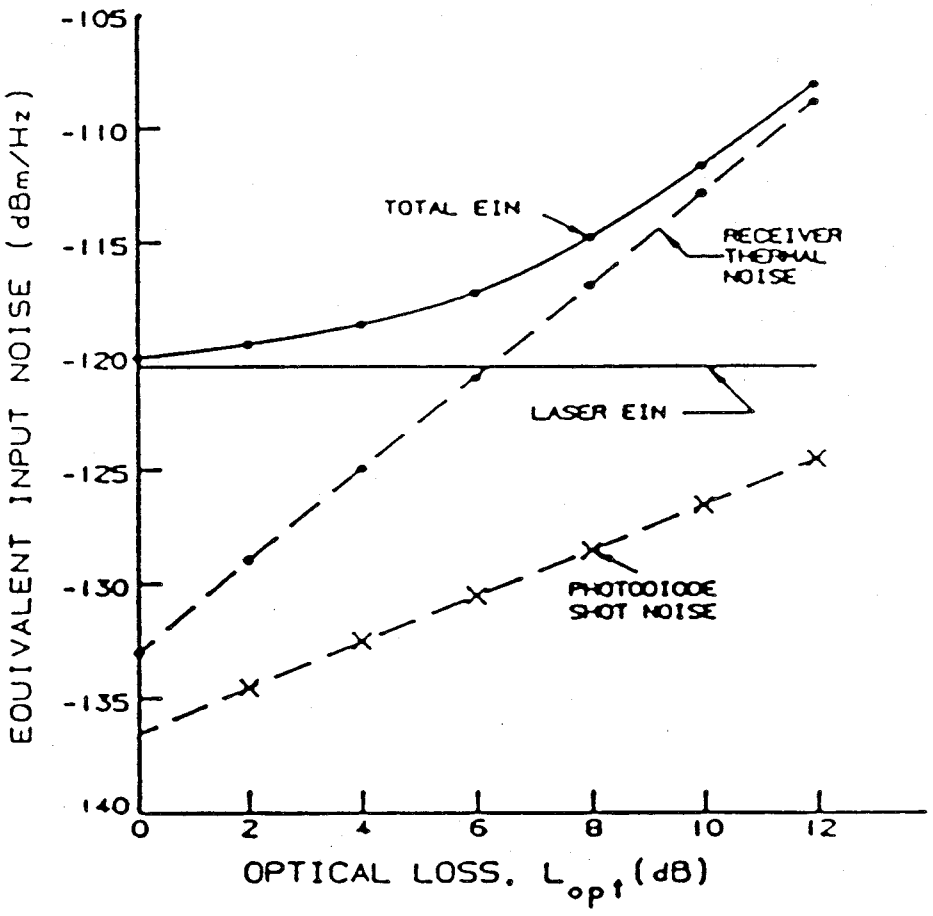

Figure 12 Total EIN versus optical loss. Typical performance for the Ortel 3510B/4510B link.

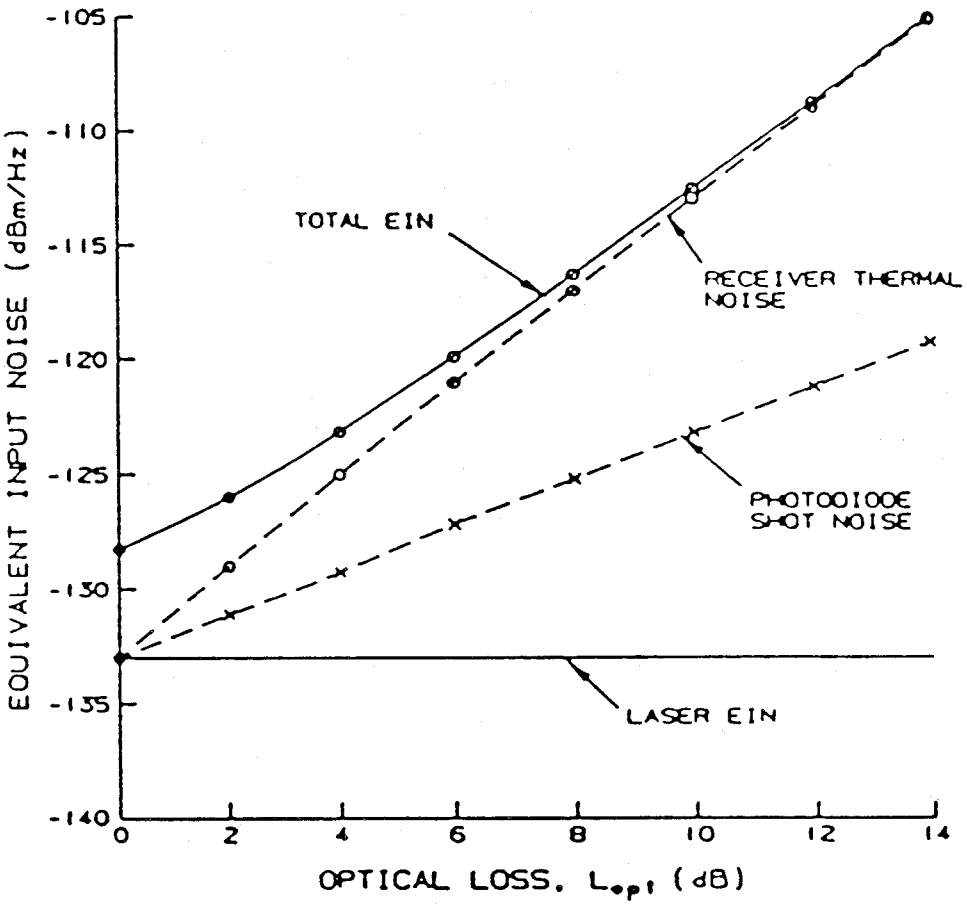

Figure 13 Total EIN versus optical loss. Typical performance for the Ortel 5515A 10 GHz link.

The sensitivity of the link is determined by noise contributions and insertion loss. For a directly modulated link, the major limiting factor was demonstrated to be the laser EIN. This implies that any post-transduction techniques for minimising link insertion loss - such as improved impedance matching or amplification (either all-optical within the fiber or conventional post-detection amplification) - will be of limited benefit since the limiting factor is the noise in the transducer itself.

3.1.6 Noise figure

The noise figure, NF, is defined as the ratio of the available noise output powers of the actual device, N_o, to that of an ideal noiseless device, N_o', of otherwise identical characteristics when the inputs are terminated by a passive load at the standard temperature of 290°K (T_o). Here,

$$N_o = [10 * \log(EIN) + 10 * \log(B)] - L_{link} \quad (dB)$$

$$N_o' = [10 * \log(k * T_o) + 10 * \log(B)] - L_{link} \quad (dB)$$

Therefore,

$$NF = N_o - N_o' \quad (dB)$$

$$= 10 * \log(EIN) + 174 \quad (dBm) \qquad (15)$$

Once the noise figure of the link is known, its contribution to the overall noise figure of a cascade of components can be calculated using Friis' formula. This formula gives the total noise figure of two cascaded transducers. Hence,

$$NF_T = NF_1 + \frac{NF_2 - 1}{G_1} \qquad (16)$$

where NF_1, G_1 = noise figure and gain of the first transducer;

NF_2 = noise figure of second transducer;

and all quantities are converted back from dB to ratios before the algebra is performed.

3.1.7 Dynamic range

The dynamic range, DR, of the fiber-optic link is a measure of the variation of signal levels that can be carried by the link. It may be defined independently of a system in two ways:

(1) It is the range from the noise floor to the input 1dB compression point. The noise floor referred to the input is given by the EIN and the bandwidth.

(2) It is also defined as the ratio of the fundamental output to the third-order intermodulation distortion (IMD) products. Since the IMD level decreases faster than the fundamental, reduction of the input signal level yields any value of DR required. However, as the input signal level decreases, the signal-to-noise ratio (SNR) also decreases because the noise out of the link is constant for a specific noise bandwidth. Thus, there is an input signal level at which the IMD level matches the noise floor, and at that input level the DR is maximized. Hence, the spurious-free dynamic range (SFDR) is the level of IMD suppression achieved when that level equals the link SNR. In Figure 14, the noise level of a hypothetical link in a 1 MHz noise bandwidth and the SFDR are also indicated. The SFDR can be calculated as [33]:

$$SFDR = (2/3) * [IP_3 - NF + 174 - 10 * \log(B)] \quad (dBm) \qquad (17)$$

where IP_3 = third-order output intercept point in dBm;

B = link bandwidth in Hz; and

NF = link-noise figure in dB.

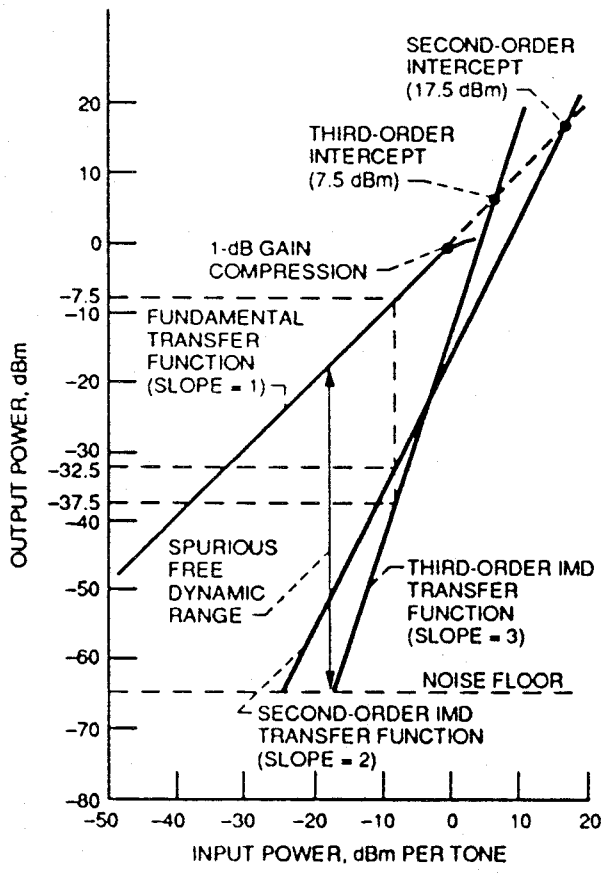

Figure 14 A typical illustration of second- and third-order intermodulation product levels, intercept points, noise floor, and SFDR for a hypothetical microwave fiber-optic link.

3.2 External modulation link

3.2.1 Insertion loss

Figure 15 shows the schematic of an externally modulated analog fiber-optic link for microwave transmission. For an externally modulated link, the insertion loss is expressed as [28],[29]:

$$L_{link} = -10*\log\{G_i*G_o*(1 - |\Gamma|^2)*R_s*R_L*[P_s*L_c*L_m*L_f*\eta_{pd}/(2*V_\pi)]^2\} \quad (dB) \quad (18)$$

where

G_i = gain of the input amplifier for the E-O modulator;

G_o = gain of the output amplifier for the E-O modulator;

Γ = reflection coefficient due to the transition between the 50 ohms line and the modulator input impedance;

R_s = source impedance;

R_L = load impedance;

P_s = optical power emitted by the laser diode;

L_c = conductor or splice loss;

L_m = optical loss through the modulator;

L_f = optical fiber loss;

η_{pd} = conversion efficiency of the photodiode (the optical power incident on the active area of the photodiode is converted into current); and

V_π = voltage for 100% modulation on electro-optic modulator.

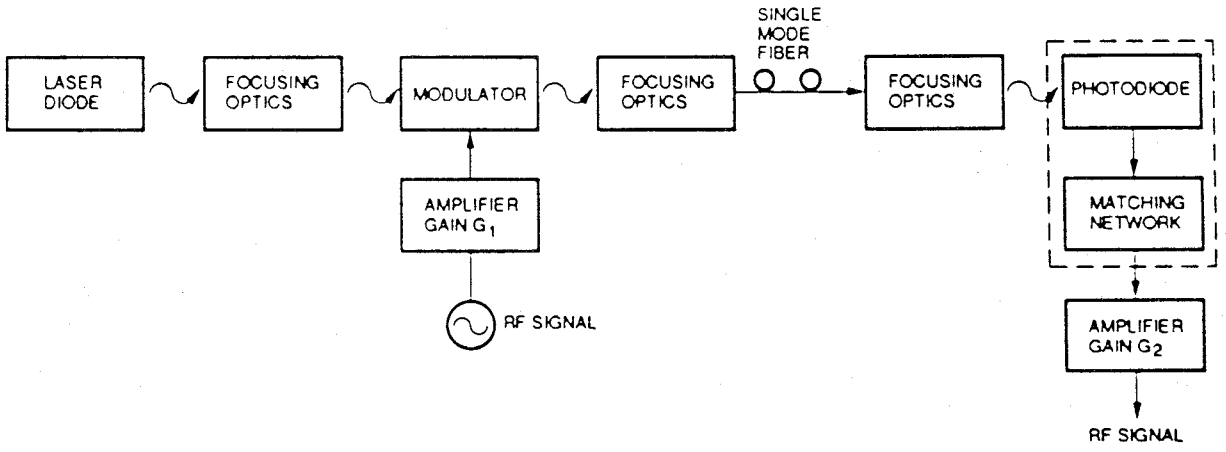

Figure 15 Schematic of an externally modulated analog fiber-optic link for microwave transmission.

3.2.2 Noise figure

The noise contributions to an externally modulated link are identical to those of the directly modulated link. However, the RIN of the laser can be made negligibly small as the laser is running cw. A typical value would be -160 dBm/Hz [11]. The thermal and shot noise contributions, given by Equation 14, are thus the major limitations to the link sensitivity, the modulator itself being a noiseless device that will only reflect the input noise due to any RF pre-amplification used. The overall link noise figure can be calculated using Equation 16.

3.2.3 Link bandwidth

Commercially available electro-optic modulators are capable of operating up to 18 GHz [34]. However, laboratory experimental electro-optic modulators with a bandwidth as high as 40 GHz [7],[8], have recently been demonstrated. At the receiver end, commercially available photodiodes are capable of direct detection up to 18 GHz [35] while laboratory experimental diodes of up to 110 GHz [36] have been demonstrated. Hence, the bandwidth requirements for most RF applications can easily be met.

For single-mode optical fibers, an additional bandwidth limitation arises due to optical fiber dispersion. Theoretically, the bandwidth-distance product of the fiber, $\Delta f*L$, is approximately given by

$$\Delta f*L = 0.44/(D_t*\sigma_\lambda) \qquad (19)$$

where Δf is the bandwidth of the fiber;

L is the total length of the fiber;

D_t is the total dispersion of the optical fiber; and

σ_λ is the rms spectral width of the optical source.

Commercially available single-mode fiber have a typical value of dispersion of about 3.5 ps/(nm*km) at 1.3 μm wavelength. This results in a bandwidth-distance product of $0.44/(3.5*10^{-12}) = 125$ GHz*km.

4 SUGGESTIONS FOR FUTURE WORK RELEVANT TO OPTICAL MICROWAVE/MILLIMETRE-WAVE INTERACTIONS

In this report, the basic concepts, characteristics, performances and applications of the fundamental microwave/millimetre-wave controlled optical devices were reviewed. In particular, methods of improving their performances, various control techniques using microwaves/millimetre-waves and limitations for such devices and components were discussed. With the recent growing interest in this area, although only a few practical devices have been implemented, rapid development in the application of lightwave technologies in microwave/millimetre-wave engineering can be expected. Several attempts have already been made to devise fast optoelectronic devices such as millimetre-wave light modulators and fast optoelectronic signal samplers. Utilization of the interaction of lightwave with submillimetre-waves and even with lightwaves will be a natural direction in the future.

As part of ongoing activities aimed at maintaining a knowledge base in electro-optical devices, it is proposed at this time to develop a millimetre-wave Electro-optic (E-O) sub-system. The specifications of such a sub-system are:

1. initial operating frequency range: 22 to 40 GHz;
2. long term operating frequency range: 90 to 110 GHz ; and
3. dynamic range: greater than 50 dB.

The development of this could be divided into three stages.

STAGE I:

The signals received from the antenna which should be capable of operating at the frequency range of 22 to 40 GHz, are first amplified and mixed to produce an intermediate frequency (I.F.) of 1 to 19 GHz. The antenna could be designed using conventional fin-line or other suitable structures, for example, groove-guide antenna. The I.F. signals produced are then amplified and used to modulate the light-carrier. Options for modulation are:

1. directly intensity-modulate the laser diode output; or
2. externally intensity-modulate the light-carrier with a modulator.

This concept has been outlined by [37]. The modulated light-carrier is then transmitted via a suitable microwave fiber-optic link and is demodulated using PIN or InGaAs type of photodiode receiver.

STAGE II:

At this stage, the operating frequency requirement would be extended to 110 GHz. Clearly, the E-O components, transmission and delay lines developed at stage I should be examined and extended for use at this frequency.

STAGE III:

The I.F. module would be removed at this stage. The signals would be amplified and used to modulate the light-carrier directly. The devices and components developed in stage II would then need to be modified due to the removal of the I.F. module.

The devices and components which require further investigation for application to the E-O sub-system are outlined below.

4.1 Modulator

What modulation method should be used for such a sub-system, Direct or External? Table 4 [28],[29] showed the performance comparison of directly modulated and externally modulated microwave fiber-optic links. Direct modulation offers simplicity, low drive power, and less overall link loss. An externally modulated link is not limited in frequency by the laser relaxation resonance and the associated relative intensity noise (RIN). However, the disadvantages of the externally modulated link include:

(a) additional coupling loss;

(b) higher drive power requirements; and

(c) more distortion.

An evaluation of the applicability of each modulation method to the receiver sub-system is required.

Two DSTO research contracts have been implemented for this work which include:

(1) appropriate modelling and characterisation techniques for laser modulation and noise properties in the multi-GHz range [27]; and

(2) design, construction and testing of a Ti:$LiNbO_3$ E-O modulator and switch [15]. The minimum 3dB bandwidth of the modulator and the switching speed between the two outputs of the switch is 3 GHz and 10 nanoseconds respectively.

The next step would be to develop an E-O modulator capable of operating in the millimetre-wave region, and incorporating these components into concept demonstrator systems. The philosophy here is to establish an "in-country" technology base in the construction and design of external modulators, so that, locally integrated optical devices can be developed. Hence, the cost of components for research needs would be lowered. Also, it would eliminate the need to import the technology, which may not be possible in the case of very high speed devices such as 40 GHz.

4.2 Switch

As with the modulator, it appears that the potential capability is sufficient to achieve extremely wide bandwidths and high sensitivities. A range of switch structures can be proposed.

4.3 Oscillator

The generation and distribution of a local oscillator signal to a number of mixers, for example, becomes progressively more difficult as the frequency is increased. An alternative to electronic oscillators is to generate a modulated laser signal in place of the RF signal and distribute it optically. There are several methods of carrying this out, two of which are:

1. the laser signal is locally modulated with the required signal frequency which can then be recovered at the point of use; and
2. the laser is used to generate the local oscillator signal directly.

The ease of distribution of the local oscillator signal, the resistance to degradation and the removal of any coupling problems into other adjacent circuitry are substantial gains for a system.

4.4 Amplifier

To amplify the modulated signals optically, the Erbium-doped fiber amplifier [38],[39] has emerged as the most effective optical amplifier for the low-loss window at around 1.55 μm wavelength. There is a possibility that the modulation distortion requirements of laser diodes can be relaxed when the Erbium-doped fiber amplifier is used as a post-amplifier. A photonic CAD model for the Erbium-doped fiber amplifier to characterise the noise processes and spectral evolution of amplified spontaneous emission (ASE) noise should be developed [26].

4.5 Detector

The aim here is to develop a wide-band, high speed, high sensitivity, high stability, reliable and cost-effective detector. In addition, the detector circuit should be compatible with other common electronics. One should consider integrating the detector and the pre-amplifier into an optical receiver as this will result in the reduction of the parasitic capacitance of the circuit and consequently may result in an improvement in the sensitivity of the receiver [10].

Instead of using a photodetector, two IMPATT diode oscillators have been used to detect intensity-modulated lightwave signals in subcarrier multiplex systems [40]. As this novel detection scheme is simple and exhibits fairly linear characteristics over a moderate band of frequencies, it may be worthwhile to further investigate the applicability of this novel detection scheme.

4.6 Filter

Several tunable filters should be considered for the proposed application. They are:

(a) Fabry-Perot interferometer filter [41];

(b) Silicon micro-machined Fabry-Perot filter [42];

(c) Bellcore's polarization-independent Acousto-Optic (A-O) phase matching filter [43];

(d) Electro-Optic (E-O) tuned filter [44];

(e) Mach-Zehnder Interferometer (MZI) filter [45]; and

(f) GaAs/AlGaAs multilayer interference filter [46].

4.7 Fiber-optic delay line

The real challenge with the delay line is to achieve a variable delay line in which the increment of delay is very small and smoothly increasable to a maximum value without great expense and rapid increase in system noise level, and very low bandwidth and dynamic range. The aim at this time is to examine the possible configurations of a microwave delay line which has a bandwidth of at least 1 GHz and a total delay of 10 microseconds achieved in increments of no more than 10 nanoseconds. The effects of dispersion and methods for optical equalization should also be investigated.

4.8 Fiber-optic link

A system model that can predict signal-to-noise ratio, non-linearity and dynamic range properties of the fiber-optic link needs to be developed. Related areas of investigation include:

1. comparison between direct modulation and external modulation schemes from a system point of view;
2. methods for reducing the insertion loss; and
3. techniques to optimise the signal-to-noise ratio of the fiber-optic link.

5 CONCLUSIONS

The basic characteristics, performances and applications of the basic devices such as laser diodes, photodetectors (PIN, APD, and photoconductive diodes), Mach-Zehnder electro-optic intensity modulators and switches fabricated on $LiNbO_3$, microwave fiber-optic delay lines and links have been reviewed. In particular, methods of improving their performances and various techniques for the microwave control of optical devices were discussed. Finally, the general characteristics have been defined for an advanced electro-optical sub-system proposed for development and areas for further investigation have been identified.

ACKNOWLEDGEMENTS

The author is grateful to David Mason for his guidance and helpful comments.

REFERENCES

[01] Pucel, R.A. (ed.),
"Monolithic Microwave Integrated Circuits",
IEEE Press, New York, 1985.

[02] Wang, G.W., and Feng, M.,
"Quarter-Micrometer Gate Ion-Implanted GaAs MESFETs with an f_t of 126 GHz",
IEEE Electron Device Letters, Vol. 10, No. 8, pp. 386-388, August 1989.

[03] Stabile, P.J., and Lalevie. B.,
"Lateral IMPATT Diodes",
IEEE Electron Device Letters, Vol. 10, No. 6, pp. 249-251, June 1989.

[04] Stabile, P.J., Rosen, A., and Herczfeld, P.R.,
"Optically Controlled Lateral PIN Diodes and Microwave Control Circuits",
RCA Review, Vol. 47, pp. 443-456, December 1986.

[05] Uomi, K., Mishima, T., and Chinone, N.,
"Ultrahigh Relaxation Oscillation Frequency (up to 30 GHz) of Highly p-doped GaAs/GaAlAs Multiple Quantum Well Lasers",
Applied Physics Letters, Vol. 51, No. 2, pp. 78-80, July 1987.

[06] Zeghbroeck, B.J.V., Patrick, W., Halbout, J.M., and Vettiger P.,
"105 GHz Bandwidth Metal-Semiconductor-Metal Photodiode",
IEEE Electron Device Letters, Vol. 9, No. 10, pp. 527-529, October 1988.

[07] Nazarathy, M., Dolfi, D.W., and Jungerman R.J.,
"Spread spectrum frequency response of coded phase reversal travelling wave modulators",
J. Lightwave Technol., Vol., LT-5, pp. 1433-1443, 1987.

[08] Dolfi, D.W., Nazarathy, M., and Jungerman R.J.,
"40 GHz Electro-Optic Modulator with 7.5V Drive Voltage",
Electronics Letters, Vol. 24, No. 9, pp. 528-529, April 1988.

[09] Vorchheimer, B. (ed.),
"Photonic and Electronic Device Technologies",
AT&T Technical Journal, Vol. 68, No. 1, January/February 1989.

[10] Hutcheson, L.D. (ed.),
"Integrated Optical Circuits and Components, Design and Applications",
Publisher: Marcel Dekker, Inc., New York and Basel, 1987.

[11] Simons, R.,
"Optical Control of Microwave Devices",
Publisher: Artech House, Boston, 1990.

[12] Lau K.Y., Chaim, N.B., Ury, I., Harder, C., and Yariv, A.,
"Direct Amplitude Modulation of Short-Cavity GaAs Lasers up to X-Band Frequencies",
Applied Physics Letters, Vol. 43, No. 1, pp. 1-3, July 1983.

[13] Wakao, K., Takagi, N., Shima, K., Hanamitsu, K., and Hori, K.I.,
"Catastrophic Degradation Level of Visible and Infrared GaAlAs Lasers",
Applied Physics Letters, Vol. 41, No. 12, pp. 1113-1115, December 1982.

[14] Blauvelt, H., Margalit, S., and Yariv, A.,
"Large Optical Cavity AlGaAs Burried Heterostructure Window Lasers",
Applied Physics Letters, Vol. 40, No. 12, pp. 1029-1031, June 1982.

[15] Austin, M.W.,
"Lithium Niobate Optical Devices",
A report for Electronic Warfare Division, Electronics Research Laboratory, Defence Science and Technology Organisation (Australia), Order No.: 25182, January 1990.

[16] Sueta, T., and Izutsu, M.,
"Integrated Optic Devices for Microwave Applications",
IEEE Trans. on MTT., Vol. 38, No. 5, pp. 477-482, May 1990.

[17] Haga, H., Izutsu, M., and Sueta, T.,
"$LiNbO_3$ travelling-wave light modulator/switch with an etched groove",
IEEE J. Quantum Electron., Vol. QE-22, pp. 902-906, 1986.

[18] Kawano, K., Kitoh, T., Jumonji, H., Nozawa, T., and Yanagibashi, M.,
"New travelling-wave electrode Mach-Zehnder optical modulator with 20 GHz bandwidth and 4.7 V driving voltage at 1.52 μm wavelength",
Electronics Letters, Vol. 25, No. 20, pp. 1382-1383, 1989.

[19] Seino, M., et al.,
"33-GHz cm broadband Mach-Zehnder modulator",
Tech. Dig., ECOC'89, pp. ThB22-5, 1989.

[20] Miura, K., Minakata, M., and Kawakami, S.,
"Perfect velocity matching of a traveling-wave integrated-optic modulator with high efficiency",
Tech. Dig., CLEO'87, April 1987.

[21] Walker, R.G.,
"High-speed electro-optic modulation in GaAs/GaAlAs waveguide devices",
J. Lightwave Technol., Vol. LT-5, pp. 1444-1453, 1987.

[22] Alferness, R.C., Korotky, S.K., and Marcatili, E.A.J.,
"Velocity-Matching Techniques for Integrated Optic Travelling Wave Switch/Modulators",
IEEE J. Quantum Electronics, Vol. QE-20, No. 3, pp. 301-309, March 1984.

[23] Kubota, K., Noda, J., and Mikami, O.,
"Travelling Wave Optical Modulator Using a Directional Coupler $LiNbO_3$ Waveguide",
IEEE J. Quantum Electronics, Vol. QE-16, No. 7, pp. 754-760, July 1980.

[24] Donnelly, J.P., and Gopinath, A.,
"A Comparison of Power Requirements of Travelling Wave $LiNbO_3$ Optical Couplers and Interferometric Modulators",
IEEE J. Quantum Electronics, Vol. QE-23, No. 1, pp. 30-41, January 1987.

[25] Komatsu, K., Yamazaki, S., Kondo, M., and Ohta, Y.,
"Low-Loss Broad-Band $LiNbO_3$ Guided-Wave Phase Modulators Using Titanium/Magnesium Double Diffusion Method",
IEEE J. Lightwave Technol., Vol. LT-5, No. 9, pp. 1239-1245, September 1987.

[26] Minasian, R.A.,
"Fibre-Optic Delay Line",
A report for Electronic Warfare Division, Electronics Research Laboratory, Defence Science and Technology Organisation (Australia), Order No.: EW 9001, 14 December 1990.

[27] Minasian, R.A.,
"High Speed Optical Fibre Link",
A report for Electronic Warfare Division, Electronics Research Laboratory, Defence Science and Technology Organisation (Australia), Order No.: EW 9002, 14 December 1990.

[28] Stephens, W.E., and Joseph, T.R.,
"System Characteristics of Direct-Modulated and Externally Modulated RF Fiber-Optic Links",
IEEE J. Lightwave Technol., Vol. LT-5, No. 3, pp. 380-387, March 1987.

[29] Cox III, C.H., Betts, G.E., and Johnson, L.M.,
"An analytic and experimental comparison of direct and external modulation in analog fiber-optic links",
IEEE Trans. on MTT., Vol. 38, No. 5, pp. 501-509, May 1990.

[30] Ortel Corporation (ed.),
"RF/Microwave Fiber Optic Link Design Guide",
Ortel Corporation, 2015 W. Chestnut Street, Alhambra, California 91803, U.S.A. [Fax: (818) 281 8231], 1988.

[31] de la Chapelle, M., and Hsu, H.P.,
"Characterization of Fiber-Optic Links for Microwave Signal Transmission",
Optical Technol. for Microwave Applications III, SPIE, Vol. 789, pp. 32-39, 1987.

[32] Browne, J.,
"Window Boosts Laser Diode Power, Ortel Corp. Product Technology",
Microwaves & RF, Vol. 24, No. 6, pp. 159-160, June 1985.

[33] Jacobi, J.H.,
"IMD: Still Unclear After 20 Years",
Microwaves & RF, Vol. 25, No. 11, pp. 119-126, November 1986.

[34] Model No.: Y-35-8808-01,
"18 GHz Integrated Optical Amplitude Modulators",
GEC Advanced Optical Products, West Hanningfield Road, Great Baddow, Chelmsford, Essex, England CM2 8HN, January 1990.

[35] Model No.: Y-35-5252,
"Ultra High Speed 18 GHz GaAs Photodiodes",
GEC Advanced Optical Products, West Hanningfield Road, Great Baddow, Chelmsford, Essex, England CM2 8HN, April 1990.

[36] Parker, D.G., Say, P.G., Hansom, A.M., and Sibbett, W.,
"110 GHz High-Efficiency Photodiodes Fabricated from Indium Tin Oxide/GaAs",
Electronics Letters, Vol. 23, No. 10, pp. 527-528, May 1987.

[37] Mason, D.B.,
"Development Task for EWT",
Subject: Group Task, Internal Minute, Electronic Warfare Division, Electronics Research Laboratory, Defence Science and Technology Organisation (Australia), File Number: NF, 7 February 1991.

[38] Urquhart, P.,
"Review of rare-earth doped fiber lasers and amplifiers",
IEE Proc. J, Opto-electronic, 135, pp. 385-407, 1988.

[39] Yoneda, E., Kikushima, K., Tsuchiya, T., and Suto, K.,
"Erbium-doped fiber amplifier for video distribution networks",
IEEE J-SAC, Vol. 8, No. 7, pp. 1249-1256, September 1990.

[40] Biswas, B.N., Bhattacharya, A.K., Mukhopadhyay, T.C., and Chaudhury, S.,
"A new possibility of detecting lightwave signals through IMPATT oscillators",
IEEE J-SAC, Vol. 8, No. 7, pp. 1387-1396, September 1990.

[41] Miller, C.M.,
"A field-worthy, high-performance, tunable fiber Fabry-Perot filter",
Proc. Euro. Conf. on Opt. Commun., September 1990.

[42] Mallinson, S.R., and Jerman, J.H.,
"Miniature micromachined Fabry-Perot interferometers in silicon",
Elect. Lett., Vol. 23, No. 20, pp. 1041-1043, September 1987.

[43] Cheung, K.W., Choy, M.M., and Kobrinski, H.,
"Electronic wavelength tuning using acousto-optic tunable filter with broad continuous tuning range and narrow channel spacing",
IEEE Phot. Tech. Lett., Vol. 1, No. 2, pp. 38-40, February 1989.

[44] Warzanskyj, W., Heismann, F., and Alferness, R.,
"Polarization-independent electro-optically tunable narrowband wavelength filter",
Appl. Phys. Lett., Vol. 53, No.1, pp. 13-15, July 1988.

[45] Toba, H., et al.,
"100-channel optical FDM transmission/distribution at 622 Mb/s over 50 km utilizing a waveguide frequency selection switch",
Elect. Lett., Vol. 26, No. 6, pp. 376-377, March 1990.

[46] Dell, J.M., and Yoffe, G.W.,
"Inline optical filter using lifted-off GaAs/AlGaAs multilayer",
Elect. Lett., Vol. 27, No. 1, pp. 26-27, January 1991.

Department of Defence

DOCUMENT CONTROL DATA SHEET

Page Classification	
UNCLASSIFED	
Privacy Marking/Caveat	

1a. AR Number	1b. Establishment Number	2. Document Date	3. Task Number
AR-006-708	ERL-0551-RR	JUNE 1991	DST 89/116

4. Title

ELECTRO-OPTIC DEVICES, COMPONENTS AND SYSTEM FOR THE MICROWAVE AND MILLIMETRE-WAVE RANGES

5. Security Classification

Document	Title	Abstract
U	U	U

S (Secret) C (Confi) R (Rest) U (Unclass)

* For UNCLASSIFIED docs with a secondary distribution LIMITATION, use (L)

6. No. of Pages	30
7. No. of Refs.	46

8. Author(s)

Dr Yat Man Choi

9. Downgrading/ Delimiting Instructions

10a. Corporate Author and Address

Electronics Research Laboratory
PO Box 1600
SALISBURY SA 5108

10b. Task Sponsor

11. Officer/Position responsible for

Security

Downgrading

Approval for release

12. Secondary Release of this Document

Approved for Public Release

Any enquiries outside stated limitations should be referred through DSTIC, Defence Information Services, Department of Defence, Anzac Park West, Canberra, ACT 2600.

13a. Deliberate Announcement

No limitation

13b. Casual Announcement (for citation in other documents)

[√] No Limitation

[ ] Ref. by Author & Doc No only

14. DEFTEST Descriptors

* Integrated optics
* Microwaves
* Millimetre waves
* Microwave/millimetre wave Monolithic Integrated Circuits

15. DISCAT Subject Codes

200601

16. Abstract

Basic characteristics, performances and designs of integrated optic devices and components for use in microwave applications and various techniques for the microwave control of optical devices are reviewed. In particular, methods of improving their performances and limitations of such devices and components are discussed. The prospects for these new technologies including recommendations for further work which are relevant to microwave and millimetre wave systems are identified.

Page Classification
UNCLASSIFED
Privacy Marking/Caveat

16. Abstract (CONT)		
17. Imprint Electronics Research Laboratory PO Box 1600 SALISBURY SA 5108		
18. Document Series and Number Research Report 0551	19. Cost Code 798067	20. Type of Report and Period Covered
21. Computer Program Used		
22. Establishment File Reference(s)		
23. Additional information (if required)		